Published in final edited form as:
Eur J Neurosci. 2006 October ; 24(7): 1885–1896. doi:10.1111/j.1460-9568.2006.05093.x.

Transplanted dopamine neurons derived from primate ES cells preferentially innervate DARPP-32 striatal progenitors within the graft

Daniela Ferrari[1,2,*], **Rosario Sanchez-Pernaute**[1,2], **Hyojin Lee**[3], **Lorenz Studer**[3], and **Ole Isacson**[1,2]

1*McLean Hospital/Harvard University Udall Parkinson's Disease Research Center of Excellence, 115 Mill St, Belmont, MA 02478, USA*

2*Neuroregeneration Laboratories, McLean Hospital, 115 Mill St, Belmont, MA 02478, USA*

3*Laboratory of Stem Cell & Tumor Biology, Division of Neurosurgery & Developmental Biology, Memorial Sloan-Kettering Cancer Center, 1275 York Ave, Box 256, New York, NY 10021, USA*

Abstract

The correct identity and functional capacity of transplanted dopamine (DA) neurons derived *in vitro* from embryonic stem (ES) cells is a critical factor for the development of an ES cell-based replacement therapy for Parkinson's disease. We transplanted primate Cyno-1 ES cells differentiated *in vitro* for 4 (progenitor ES cells) or 6 (differentiated ES cells) weeks, or control fetal primate cells into the striatum of hemi-parkinsonian rats. Partial behavioral recovery in amphetamine-induced rotation was correlated with the number of ES-derived tyrosine hydroxylase-positive (TH +) neurons in the grafts ($r = 0.5$, $P < 0.05$). *Post mortem* analysis of ES-derived grafts revealed TH + neurons with mature morphology, similar to fetal DA neurons, and expression of midbrain transcription factors, such as Engrailed (En) and Nurr-1. While the total number of TH + neurons was not different between the two groups, TH/En co-expression was significantly higher (> 90%) in grafts from differentiated ES cells than in grafts derived from progenitor cells (< 50%), reflecting a more heterogeneous cellular composition. Within the grafts there was an overlap between ES-derived TH + axonal arbors and clusters of primate ES-derived striatal neurons expressing brain factor 1 (Bf-1, Foxg1) and DA and cAMP-regulated phosphoprotein (DARPP-32). Such overlap was never observed for other regional transcription factors that define neighboring forebrain domains in the developing brain, such as Nkx2.1 (medial ganglionic eminence), Nkx2.2 (pallidal and diencephalic progenitors) or Pax6 (dorsal telencephalic progenitors). Despite the heterogeneity of ES-derived graft cell composition, these results demonstrate normal phenotypic specification, conserved natural axonal target selectivity and functionality of DA neurons derived from primate ES cells.

Keywords

dopamine; embryonic stem cells; Parkinson's disease; striatum; transplantation

Correspondence: Dr R. Sanchez-Pernaute or Dr O. Isacson, Neuroregeneration Laboratories, McLean Hospital, 115 Mill St, Belmont, MA 02478, USA. E-mail: rosario_pernaute@hms.harvard.edu or isacson@hms.harvard.edu.
*Present address: Stem Cell Research Institute, DIBIT, S. Raffaele Hospital, Via Olgettina 58, 20132 Milano, Italy

Introduction

Dopamine (DA) neurons can be obtained from human and primate embryonic stem (ES) cells using different strategies (Reubinoff *et al*., 2001; Ben-Hur *et al*., 2004; Perrier *et al*., 2004; Sanchez-Pernaute *et al*., 2005; Takagi *et al*., 2005; Yan *et al*., 2005). *In vivo*, survival and, subsequently, function of these DA neurons following transplantation into rodents and primates has been limited (Ben-Hur *et al*., 2004; Park *et al*., 2005; Sanchez-Pernaute *et al*., 2005; Takagi *et al*., 2005; Brederlau *et al*., 2006).

Our *in vitro* inductive differentiation protocol (Perrier *et al*., 2004; Sanchez-Pernaute *et al*., 2005) recapitulates the regionalization process at the midbrain organizer during embryonic development by exposing the cells after neural induction to sonic hedgehog (SHH) and fibroblast growth factor (FGF) 8 (Ye *et al*., 1998). These two molecules are also required for induction of ventral forebrain (Echevarria *et al*., 2003) and, *in vivo*, we have described that a majority of primate cells expressed the forebrain transcription factor, brain factor 1 (Bf-1 or Foxg-1) (Sanchez-Pernaute *et al*., 2005). Importantly, the lateral ganglionic eminence (LGE) where the medium-size spiny striatal neurons [the target of ventral midbrain (VM) DA neurons] originate is located within the Bf-1-positive domain in the developing telencephalon, together with the medial ganglionic eminence and the pallium (Tao & Lai, 1992). Forebrain subregionalization is characterized by timed expression of certain transcription factors (Corbin *et al*., 2003), such as Nkx2.1 and Nkx2.2, which are developmentally regulated and can be used to identify progenitor and neuronal populations.

In this study we show that DA neurons generated from primate parthenogenetic ES cells can compensate motor asymmetry and express *in vivo* typical midbrain transcription factors and phenotypic markers. Further supporting the correct specification of these ES-derived DA neurons, we provide evidence of appropriate innervation by ES-derived midbrain-like DA neurons of their natural developmental target, the striatal neural progenitors present in the grafts.

Materials and methods

ES cell propagation and differentiation into DA neurons

The experiments were performed using the primate parthenogenetic ES cell line Cyno-1 kindly provided by J. Cibelli, Michigan State University (Cibelli *et al*., 2002; Vrana *et al*., 2003). In order to induce differentiation of ES cells into midbrain DA neurons, we used the protocol described in our recent study (Sanchez-Pernaute *et al*., 2005). Briefly, cells were plated on a confluent layer of irradiated (50 Gy) stromal feeder cell line (MS5) and grown in serum replacement medium. At day 9, SHH (200 ng/mL) and FGF8 (100 ng/mL) were added to the medium. After 12 days cultures were switched to N2 medium modified according to Johe *et al*. (1996) in the presence of SHH, FGF8, brain-derived neurotrophic factor (BDNF; 20 ng/mL) and ascorbic acid (AA, 0.2 mM). At day 16, SHH and FGF8 were withdrawn until day 21. At day 21, rosettes structures containing neural precursors were manually isolated and replated on polyornithine (15 μg/mL)/laminin (1 μg/mL)-coated culture dishes in N2 medium supplemented with SHH, FGF8, AA and BDNF. After 1 week, cells were mechanically passaged and replated in the same conditions for 7 additional days. Cells were finally differentiated in the presence of BDNF, glial-derived neurotrophic factor (GDNF; 10 ng/mL), dibutyryl cAMP (1 mM) and AA for 1 week.

6-Hydroxydopamine (6-OHDA) lesion and behavioral analysis

All animal studies were performed following NIH guidelines, and were approved by the IACUC at McLean Hospital and HMS. 6-OHDA-lesioned adult female Sprague–Dawley rats

(200–250 g) were purchased from Charles River Laboratories and Taconic. The animals were unilaterally lesioned by 6-OHDA injection (8 μg, 2 μg/μL/min) into the medial forebrain bundle (AP −4.3, Lat −1.2, DV −8.3) under sodium pentobarbital anesthesia. Rotational behavior in response to amphetamine (4 mg kg i.p.) was evaluated before and after 6, 9 and 11 or 12 weeks post-transplantation. Animals were placed (randomized) into automated rotometer bowls, and left and right full-body turns were monitored by a computerized activity monitor system.

Animals showing > 700 turns ipsilateral to the lesioned side in 90 min after a single dose of amphetamine (average 12.7 ± 0.9 turns/min) were selected for transplantation.

Cell preparation and transplantation

We transplanted Cyno-1 cells, at two maturation stages along the described differentiation protocol, at day 28 (progenitors, pES) and 42 (differentiated neurons, dES). For each maturation stage we transplanted two groups of animals: one received cells pretreated with mitomycin C, 1 μg/mL, for 90 min at 37 °C (pES $n = 11$ and dES $n = 8$) and the other was transplanted with untreated cells (pES $n = 10$ and dES $n = 8$). To reduce the number of proliferative cells in the untreated pES, rosettes were manually removed from the dish before harvesting the cells for transplantation. Cells were harvested without enzymatic digestion and mechanically dissociated into a cell suspension. Acridine orange/ethidium bromide staining was used to assess cell viability. Cells were counted, re-suspended at ~25 000 viable cells/μL in the final differentiation medium, and 100 000 cells were injected into two AP sites in the lesioned striatum of the rats (AP 0.6 lat −2.8 and AP −0.6 lat −3.2 from bregma, and from −5.5 to −4.5 mm ventral from dura, with the tooth bar set at −3.3). Injections were performed as previously described (Kim *et al*., 2002) under ketamine/xylazine anesthesia. For each session an aliquot from the cell suspension was re-plated in polyornithine/laminin-coated coverslips for further characterization.

The following control groups were used: fetal primate DA cell transplantation ($n = 3$, fetal VM), fetal primate striatal cell transplantation ($n = 4$, fetal LGE) and sham (no cells, $n = 3$). Fetal tissue was obtained from 6–7-week-old Cynomolgus monkey embryos from the UC Davis Regional Primate Center. VM and LGE dissection was performed as described (Galpern *et al*., 1996), and 3 μL of the VM cell suspension (~ 30 000 cells/μL; 90 000 cells; 96% cell viability) or LGE cell suspension (50 000 cells/μL) was injected in the striatum of 6-OHDA-lesioned rats, at AP 0.5, lat −3 and ventral −5 to −4 (Paxinos & Watson, 1986). Rotations (at 6, 12 and 16 weeks) and *post mortem* analysis was performed as described for ES grafts.

To prevent rejection of grafted primate cells, all rats were immunosuppressed with cyclosporin A (15 mg/kg/day, Sandimmune, Sandoz, East Hannover, NJ, USA) starting 1 day prior to surgery. After 10 weeks, the dose of cyclosporin was reduced to 10 mg/kg/day.

Immunohistological and stereological procedures

Animals were terminally anesthetized with an i.p. overdose of pentobarbital (150 mg/kg), and perfused intracardially with 70 mL heparinized saline (0.1% heparin in 0.9% saline) followed by 100 mL paraformaldehyde [4% in phosphate-buffered saline (PBS)]. Brains were removed, postfixed for 4 h in 4% paraformaldehyde, equilibrated in sucrose (20% in PBS) and sectioned on a freezing microtome in 40-μm slices that were serially collected. Donor cells were identified in the rodent by using two primate-specific antibodies: human nuclear antigen (HNA) 1 : 50, Chemicon, Temecula, CA, USA; and a primate-specific neural cell adhesion molecule (NCAM) (clone eric1, 1 : 100, Santa Cruz Biotechnology, Santa Cruz, CA, USA). Characterization of grafted cell phenotypes was performed using multiple immunofluorescence labeling with the following primary antibodies: Engrailed 1/2 (En, clone 4G11; 1 : 20), Islet-1 (Isl-1; 39.4D5, 1 : 100) and Nkx2.2 (all monoclonal raised in mouse)

were purchased from the Developmental Studies Hybridoma Bank (DSHB, Iowa City, IA, USA). Neuronal nuclei (NeuN; 1 : 100, mouse), aromatic amino acid decarboxylase (AADC; 1 : 200, sheep) and DA transporter (DAT; 1 : 500, rat), Neurofilament 70 (NF70; 1 : 100 mouse), DA and cAMP-regulated phosphoprotein (DARPP-32; 1 : 1000, rabbit) were from Chemicon; tyrosine hydroxylase (TH; 1 : 250, rabbit or sheep), vesicular monoamine transporter (VMAT-2; 1 : 300, rabbit) were from Pel-Freez Biologics (Rogers, AR, USA); G-coupled inward rectifier K channel (Girk-2; 1 : 400, goat), Nkx2.1 (TTF1; 1 : 100, rabbit), Nurr-1 (N-20, 1 : 100, rabbit), doublecortin (1 : 250, guinea pig) and PCNA (1 : 100, mouse) were from Santa Cruz; Calbindin-D28k (1 : 2000, mouse) was from Swant (Switzerland); Bf-1 (rabbit polyclonal, 1 : 500) was a gift from Dr Lai; neuron-specific class III β-tubulin (clone TuJ1; 1 : 1000, rabbit or mouse) was purchased from Covance (Berkeley, CA, USA).

Sections were permeabilized with 0.1% Triton X-100 and incubated with primary antibodies in 10% normal serum overnight at 4 °C; after rinsing, sections were incubated in fluorescence-labeled secondary antibodies (Molecular Probes, Eugene, OR, USA, 1 : 500) for 1 h at room temperature, rinsed and incubated with Hoechst 33342 (4 μg/mL). For light microscopy, biotinylated secondary antibodies (Vector Laboratories, Burlingame, CA, USA; 1 : 300) were used, followed by incubation in streptavidin-biotin complex (Vectastain ABC Kit Elite, Vector Laboratories) for 60 min at room temperature and visualized by incubation in 3,3′-diaminobenzidine solution with nickel enhancement (Vector Laboratories). Antigen retrieval was performed by preincubating the sections in target retrieval solution (Dako) for 20 min at 85 °C. Control experiments were performed by omission of primary antibodies and by using a different combination of fluorescent secondary antibodies from Molecular Probes.

Confocal analysis was performed using a Zeiss LSM510/Meta station (Thornwood, NY, USA). For identification of signal co-localization within a cell, optical sections were kept to a minimal thickness and orthogonal reconstructions were obtained.

Quantitative analysis was performed by systematic evaluation of series of sections (240–480 μm apart) spanning the grafts using Stereo Investigator image capture equipment and software (MicroBright-Field, Williston, VT, USA). Graft volumes were calculated using the Cavalieri estimator probe. The coefficient of error was used to assess probe accuracy and $P < 0.05$ was considered acceptable. The areas of DARPP-32-and TH-positive regions were calculated using Neuroexplorer (MicroBrightField). Cell counts of TH + and DARPP-32 + neurons were performed on every sixth (TH) or 12th (DARPP32) section using an Axioplan microscope (Zeiss) under a 40 × lens. Only stained cells with visible dendrites were counted as neurons, and counts from serial sections were corrected and extrapolated for whole graft volumes using the Abercrombie method (Abercrombie, 1946). Estimation of co-expression of En/TH, calbindin/DARPP-32 and Isl-1/DARPP-32 was assessed in random fields in all available sections containing the graft within one series (~ 500 cells) in four dES grafts and three–four pES, and results are expressed as percentages. HNA staining was used to delineate the graft borders and to confirm the identity of the primate neurons at the graft/host interface.

All data are presented as mean ± SEM. Simple regression analyses were performed to evaluate the correlation between behavioral recovery and surviving TH + neurons. Comparisons between the groups were performed using one-way ANOVA, and the effect of the graft on amphetamine rotation over time was evaluated using repeated-measures ANOVA. Statistical analyses were performed using Statview software (SAS Institute, Carny, NC, USA).

Results

ES cell differentiation

We used a sequential induction protocol (Sanchez-Pernaute *et al*., 2005) to differentiate primate ES cells into midbrain-like DA neurons and transplanted the cells at two maturation stages, at day 28 (progenitors, pES) and day 42 (differentiated neurons, dES). At both stages, half of the cell culture dishes were treated with mitomycin C immediately before harvesting, as described (Sanchez-Pernaute *et al*., 2005). For each cell preparation used for transplantation, control cells were re-plated on glass coverslips and fixed 3 days later for immunohistochemistry. After replating, there was no significant difference in the number of TH + neurons (~ 1–2% of the total cell number) between the two stages, but TH + neurons present in cultures prepared from pES cells displayed shorter and less branched neurites than dES (data not shown).

Transplantation and functional analysis

For each ES cell preparation a total of 100 000 cells were transplanted into the striatum of hemi-parkinsonian, 6-OHDA-lesioned rats. Rats were tested for D-amphetamine-induced rotation before and 6, 9 and 12 weeks post-transplantation (Fig. 1A and B). Control experiments using fetal primate cells showed a progressive reduction of rotation 3–4 months after transplantation of fetal VM (Fig. 1C), while cells from the LGE (Fig. 1C) had no effect. Roughly 50% of the animals grafted with pES and 80% of the rats receiving dES showed some degree of improvement (Fig. 1A and B). Based on previous data demonstrating the requirement of graft survival with a minimum number of surviving DA neurons for functional response to D-amphetamine −120–400 (Brundin *et al*., 1985, 1988a; Galpern *et al*., 1996; Annett *et al*., 1997), only animals (from all shown in Fig. 1A and B) that had ≥ 200 TH + cells in the *post mortem* analysis are included in Fig. 1C. In this subgroup ($n = 15$), the behavioral recovery at 12 weeks was similar to that seen with rats receiving fetal primate VM grafts (Fig. 1C), and the number of TH + neurons in the graft correlated with the improvement in amphetamine rotation ($r = 0.5$, $P = 0.05$). This correlation was higher ($r = 0.73$, $P < 0.05$) if we considered only dES grafted animals, in which there was no graft overgrowth that can interfere with motor performance.

Graft morphology and DA phenotype

All animals receiving pES had surviving grafts in the *post mortem* analysis, while graft survival was slightly lower (14/16) in the group receiving dES. Transplantation of pES resulted in the formation of very large grafts. Average graft volumes were measured on HNA staining and were slightly smaller for pES cells treated with mitomycin C (52 ± 8 mm^3) than for pES cells untreated before grafting (71.6 ± 6 mm^3, $F_{1,19} = 4$, $P = 0.06$). This group of animals was killed before the end of the study (11 weeks) because some animals ($n = 4$) presented with lethargy, hemiparesis or weight loss. Some of these grafts were morphologically heterogeneous and contained pockets of PCNA + proliferative cells that did not co-express neural markers, including NeuN, NCAM, doublecortin, TuJ1 and glial fibrillary acidic protein (GFAP; data not shown), which were otherwise ubiquitously expressed. As we have previously reported (Sanchez-Pernaute *et al*., 2005), proliferation of primate forebrain neural progenitors after transplantation may result in large compressive grafts. However, we cannot exclude that, in some cases, pES grafts contained non-neural cells. Grafts from dES were significantly smaller (2.4 ± 1 and 5.9 ± 1 mm^3 with and without mitomycin C, respectively), and the effect of mitomycin C pretreatment was significant ($F_{1,12} = 8.7$, $P = 0.01$). No graft overgrowths were observed in animals receiving dES.

In transplants derived from fetal primate VM, TH + neurons (Fig. 2) were located in clusters, close to the graft–host interface with large polygonal somas and complex neuritic branches (Fig. 2B). TH + neurons were co-localized with the primate-specific marker NCAM clone eric1

(Fig. 2C) and expressed VMAT-2 (Fig. 2D). TH + neurons from fetal (Fig. 2B) and ES origin (Fig. 3A and B) displayed similar morphology with large cell bodies (18–20 μm) arranged in clusters in the periphery of the graft and extensive fiber growth. TH + neurons co-expressed the primate-specific nuclear antigen HNA (Fig. 3C), the neuronal marker NeuN (Fig. 3D) and typical DA markers such as VMAT-2 (Fig. 3E), AADC and DAT (Sanchez-Pernaute *et al*., 2005; and not shown). TH + neurons expressed the midbrain-specific homeobox transcription factor Engrailed (En) (Fig. 3F and G). In dES grafts 93 ± 3% of TH + neurons expressed En, while in pES grafts co-expression of TH and En was significantly lower (42 ± 7%; $F_{1,5} = 49$, $P < 0.001$), reflecting the presence of several DA subpopulations and the heterogeneous composition of the grafts. A subset of TH + neurons co-expressed Girk-2 (Fig. 3I), which is preferentially expressed in midbrain DA neurons in the substantia pars compacta (Mendez *et al*., 2005). Likewise, other TH + neurons co-expressed calbindin, which is found in midbrain subpopulations integrated in the limbic system (Fig. 3J and K). As we have observed in human fetal VM grafts and has been reported also for murine fetal VM, the TH/calbindin neurons were located medially in the graft (Fig. 3J) while TH/Girk-2 were more often located at the host–graft interface. Other calbindin + neurons were present in the graft, but were not particularly abundant in the TH + areas (see below).

There were no significant differences in the number of TH + neurons present in the grafts derived from pES and dES (344 ± 75, 225 ± 64, $P > 0.5$). There was, however, a significant effect of mitomycin C, which resulted in a reduction of TH + neurons survival (113 ± 30 and 418 ± 73, $F_{1,22} = 14.8$, $P < 0.001$), as in our previous study (Sanchez-Pernaute *et al*., 2005).

Qualitative and quantitative analysis of TH + fiber growth

TH + fibers from transplanted dES neurons sometimes grew towards the host and innervated nearby striatal areas (Fig. 4A and B). This outgrowth was also observed in grafts derived from pES (Fig. 5A and B) in spite of disruptive graft overgrowth. However, in all the grafts, patches of very dense TH + axonal arborization were found within the graft (Fig. 4B asterisks and Fig. 5C and D). To identify the attractant factors directing such self-innervation or ingrowth and its functional relevance, we performed additional immunohistochemical characterization and quantitative analysis of these areas.

Grafted cells within the TH + highly innervated patches were positive for neuronal markers (NeuN, neurofilament NF70, Fig. 6A and B) and expressed the forebrain transcription factor Bf-1 (Foxg-1) (Figs 4C and 5E). However, Bf-11 expression was high also in contiguous areas that did not receive TH + axons (Fig. 4C), indicating that only a subclass of Bf-1 + (forebrain) neuronal progenitors was attracting TH + neurites. We found a strong co-localization between TH + fibers and Bf-1 + DARPP-32 + neurons (Fig. 4F). DARPP-32 is a DA and cyclic AMP-regulated phosphoprotein expressed by LGE progenitors during development and in medium-size spiny neurons in the adult striatum (Fig. 4J). TH + fibers were preferentially, but not exclusively, directed towards graft-derived (co-expressing HNA, Figs 4G and H, and 7A–C) DARPP-32 + neurons (Figs 4D and E, 7A–C, and 5F, pES) and not to DARPP-32 + neurons in the host striatum (Figs 4D, 7C and 5C). The DARPP-32 + neurons within the graft hardly ever co-expressed calbindin (Fig. 4I), while co-expression of calbindin by mature DARPP-32 + host striatal neurons was ubiquitous (Fig. 4I). DARPP-32 + neurons in the grafts often co-expressed Isl-1 (Figs 4K and L, and 5F), which is present in LGE progenitors early during development, and is downregulated in adult medium-size spiny neurons while maintained in large cholinergic interneurons (Fig. 4J, arrow) (Wang & Liu, 2001; Chang *et al*., 2004). The absence of calbindin and co-expression of Isl-1 by DARPP-32 + neurons indicated that these neurons were still immature (Wang & Liu, 2001; Chang *et al*., 2004).

We next examined the expression of several transcription factors that are associated with forebrain regionalization. We failed to identify any specific pattern of distribution in areas with

dense TH + fibers for cells expressing Nkx2.2 (diencephalic progenitors), Nkx2.1 (ventral forebrain medial ganglionic eminence) or Pax6 (dorsal telencephalic progenitors) (Fig. 6C and D, and not shown). These results indicate that TH + neurons selectively innervated the LGE neurons that were present within the graft (HNA +, Figs 6E and 7A–C).

Quantification of the number of DARPP-32 + progenitors in the graft and their relation with TH + fibers was performed in animals transplanted with dES ($n = 8$). Using stereological software (Stereo Investigator) we generated maps of the distribution of DARPP-32 + clusters with respect to the TH + innervation for each animal of this group. Areas densely covered by thin TH + fibers (Fig. 7A, light gray areas in maps in Fig. 7D and E) occupied between 14 and 44% of the graft area. These areas did not include TH + cell bodies and thick sparse branches (mapped in dark gray in Fig. 7D and E), which represented between 3 and 21% of the total graft area. Topographically, the clusters of DARPP-32 + neurons coincided with areas of TH + innervation (> 95% $n = 8$, Fig. 7F).

Discussion

In this study we found that transplanted primate Cyno-1 pES-and dES-derived DA neurons can mitigate motor asymmetry in the 6-OHDA rat model of Parkinson's disease. Three months after transplantation the rats with successful ES-derived grafts recovered at a rate similar to primate fetal-derived VM neurons. ES-derived TH + neurons displayed typical morphology, and expressed midbrain DA transcription factors (Simon *et al*., 2003) and characteristic phenotypic markers of VM DA subpopulations (Mendez *et al*., 2005; Thompson *et al*., 2005). dES grafts contained almost exclusively midbrain DA neurons (expressing En), while pES grafts had more diverse DA subpopulations (En +/−). Two recent studies have shown that longer *in vitro* culture times reduce the likelihood of teratoma formation from mouse (Fukuda *et al*., 2006) and human ES cells (Brederlau *et al*., 2006). In this study we found that pES grafts (28 days *in vitro*) were larger and more heterogeneous than dES grafts (42 days *in vitro*), and contained clusters of proliferating cells that did not express neural markers at the time of analysis. However, rapid expansion of primate forebrain neural precursors can also result in large grafts (Sanchez-Pernaute *et al*., 2005). Grafts from pES and dES were different from fetal VM grafts, where all the donor cells in the graft have a similar regional specification. In contrast, ES-derived grafts contained more diverse neuronal populations, with different regional identity. In fact, our data demonstrate that ES-derived grafts resembled, in some aspects, fetal VM/LGE co-grafts.

DA axonal growth target specificity

Transplanted fetal neurons selectively re-innervate specific targets in the host brain (Schultzberg *et al*., 1984; Isacson *et al*., 1995, 2003; Isacson & Deacon, 1996; Thompson *et al*., 2005), and fetal midbrain DA neurons are capable to form appropriate synaptic connections with medium-size spiny striatal neurons (Clarke *et al*., 1988), their primary target. Axonal target specificity involves both target-derived trophic support and cell contact recognition of cell surface molecules (Tessier-Lavigne & Goodman, 1996), and neuronal identity is intimately linked to specific axonal path choices. Our analysis revealed that ES-derived DA neurons preferentially innervated graft areas with clusters of developing LGE neurons, the natural developmental target of midbrain DA neurons.

The presence of DARPP-32 immature neurons within the ES-derived grafts may have contributed to robust axonal growth and arborization of the DA cells while, at the same time, potentially interfering with outgrowth. During development, expression of DARPP-32 precedes the arrival of TH + fibers and may act to attract or stabilize incoming TH innervation (Foster *et al*., 1987). *In vitro* studies have shown potent trophic and tropic effects of striatal tissue and extracts on nigral DA neuron survival and function in different co-culture systems

(Prochiantz *et al*., 1979, 1981; di Porzio *et al*., 1980; Hemmendinger *et al*., 1981; Foster *et al*., 1987). Such effects have also been documented *in vivo* in studies using co-transplantation paradigms into the adult brain (Brundin *et al*., 1986; de Beaurepaire & Freed, 1987; Yurek *et al*., 1990; Costantini & Snyder-Keller, 1997; Sortwell *et al*., 1998). In those studies, the presence of fetal LGE cells in the graft seemed to improve DA neuron survival and promote axonal extension, as *in vitro*. The *in vivo* graft situation provides two striatal targets, one adult and one fetal, that can result in 'hyperinnervation' or 'ingrowth' of DA axons into the fetal LGE (Brundin *et al*., 1986; de Beaurepaire & Freed, 1987; Costantini & Snyder-Keller, 1997; Sortwell *et al*., 1998). In previous co-graft studies the effects on functional outcome were not marked (Yurek *et al*., 1990; Emgard-Mattson *et al*., 1997; Sortwell *et al*., 1998). In this study we found that the densest patches of TH + fibers were located within the graft, in a very similar way to the dense and patchy DA hyperinnervation of the striatal component of the graft in the aforementioned fetal co-graft experiments. As described for fetal VM/LGE co-grafts in the eye (Stromberg *et al*., 1997) and in other transplantation paradigms (Holm & Isacson, 1999), the attraction between axon and target is predicated on the interplay between factors related to developmental stages and donor–host age match. Our results demonstrate that axonal target selectivity is maintained by DA neurons derived from ES cells with a preference for their isochronic target, LGE, over the mature (anisochronic) host striatum.

Functional capacity of transplanted neurons

The correction of motor asymmetry was only apparent with the presence of ≥ 200 TH + neurons in the grafts. DA cell numbers, fiber outgrowth, graft composition and other factors such as location and host immune response can modulate the outcome of transplants (Dunnet *et al*., 1983; Brundin *et al*., 1988b; Mandel *et al*., 1990; Isacson *et al*., 1998). DA neurons derived from mouse ES cells are capable of restoring motor function in the rat hemi-parkinsonian model (Bjorklund *et al*., 2002; Kim *et al*., 2002) in a similar way to fetal VM DA neurons. However, these murine functional grafts contained thousands of DA neurons. A recent study (Yurek & Fletcher-Turner, 2004) directly compared the effects of mouse fetal and ES-derived DA neurons in grafts containing similar low numbers of DA neurons. ES cell-derived DA neurons appeared somewhat less efficient but, unfortunately, the latest time point examined in that study was 4 weeks and it is possible that neurons derived from ES cells require more time to mature (Bjorklund *et al*., 2002). In contrast, our data do not support the idea that DA neurons derived from ES cells have limited functional capacity (Bjorklund *et al*., 2002; Kim *et al*., 2002). In recent studies survival of grafted DA neurons derived from human and primate ES cells, and therefore behavioral improvement, was rather limited (Buytaert-Hoefen *et al*., 2004; Schulz *et al*., 2004; Park *et al*., 2005; Sanchez-Pernaute *et al*., 2005; Brederlau *et al*., 2006). Here we demonstrate that DA neurons derived from primate ES cells can compensate, when graft survival is sufficient, amphetamine-induced rotation.

In conclusion, transplanted DA neurons derived *in vitro* from primate parthenogenetic ES cells have characteristics similar to fetal VM neuroblasts, can function *in vivo* and show a correct midbrain phenotype and specific axonal target selection. However, ES-derived grafts have much more tissue heterogeneity than the fetal regionally specified DA neurons. Sequential exposure *in vitro* to inductive signals, as in this protocol, results in a relative enrichment in midbrain DA neurons, but it is not sufficient to obtain an adequate population for cell replacement therapies. Further selection and cell purification steps are therefore required for a cell therapy based on ES-derived DA neurons.

Acknowledgements

This work was supported by the Harvard Stem Cell Institute; NINDS P50 NS-39793; N.E.R.P.R.C. Center Grant P51RR00168. Support from the Orchard Foundation, Vaughan Foundation, Michael Stern Parkinson Foundation and

Consolidated Anti Ageing Foundation is greatly appreciated. D.F. is a fellow of the Vita-Salute San Raffaele University PhD program.

References

Abercrombie M. Estimation of nuclear populations from microtome sections. Anat Rec 1946;94:239–247.

Annett LE, Torres EM, Clarke DJ, Ishida Y, Barker RA, Ridley RM, Baker HF, Dunnett SB. Survival of nigral grafts within the striatum of marmosets with 6-OHDA lesions depends critically on donor embryo age. Cell Transplant 1997;6:557–569. [PubMed: 9440865]

de Beaurepaire R, Freed WJ. Embryonic substantia nigra grafts innervate embryonic striatal co-grafts in preference to mature host striatum. Exp Neurol 1987;95:448–454. [PubMed: 3100320]

Ben-Hur T, Idelson M, Khaner H, Pera M, Reinhartz E, Itzik A, Reubinoff BE. Transplantation of human embryonic stem cell-derived neural progenitors improves behavioral deficit in Parkinsonian rats. Stem Cells 2004;22:1246–1255. [PubMed: 15579643]

Bjorklund LM, Sanchez-Pernaute R, Chung S, Andersson T, Chen IY, McNaught KS, Brownell AL, Jenkins BG, Wahlestedt C, Kim KS, Isacson O. Embryonic stem cells develop into functional dopaminergic neurons after transplantation in a Parkinson rat model. Proc Natl Acad Sci USA 2002;99:2344–2349. [PubMed: 11782534]

Brederlau A, Correia AS, Anisimov SV, Elmi M, Paul G, Roybon L, Morizane A, Bergquist F, Riebe I, Nannmark U, Carta M, Hanse E, Takahashi J, Sasai Y, Funa K, Brundin P, Eriksson PS, Li JY. Transplantation of human embryonic stem cell-derived cells to a rat model of Parkinson's disease: effect of in vitro differentiation on graft survival and teratoma formation. Stem Cells 2006;24:1433–1440. [PubMed: 16556709]

Brundin P, Barbin G, Strecker RE, Isacson O, Prochiantz A, Bjorklund A. Survival and function of dissociated rat dopamine neurones grafted at different developmental stages or after being cultured in vitro. Brain Res 1988a;467:233–243. [PubMed: 3378172]

Brundin P, Isacson O, Björklund A. Monitoring of cell viability in suspensions of embryonic CNS tissue and its use as a criterion for intracerebral graft survival. Brain Res 1985;331:251–259. [PubMed: 3986568]

Brundin P, Isacson O, Gage F, Bjorklund A. Intrastriatal grafting of dopamine-containing neuronal cell suspensions: effects of mixing with target or non-target cells. Brain Res 1986;389:77–84. [PubMed: 3081240]

Brundin P, Strecker RE, Widner H, Clarke DJ, Nilsson OG, Astedt B, Lindvall O, Bjorklund A. Human fetal dopamine neurons grafted in a rat model of Parkinson's disease: immunological aspects, spontaneous and drug-induced behaviour, and dopamine release. Exp Brain Res 1988b;70:192–208. [PubMed: 3402564]

Buytaert-Hoefen KA, Alvarez E, Freed CR. Generation of tyrosine hydroxylase positive neurons from human embryonic stem cells after coculture with cellular substrates and exposure to GDNF. Stem Cells 2004;22:669–674. [PubMed: 15342931]

Chang CW, Tsai CW, Wang HF, Tsai HC, Chen HY, Tsai TF, Takahashi H, Li HY, Fann MJ, Yang CW, Hayashizaki Y, Saito T, Liu FC. Identification of a developmentally regulated striatum-enriched zinc-finger gene, Nolz-1, in the mammalian brain. Proc Natl Acad Sci USA 2004;101:2613–2618. [PubMed: 14983057]

Cibelli JB, Grant KA, Chapman KB, Cunniff K, Worst T, Green HL, Walker SJ, Gutin PH, Vilner L, Tabar V, Dominko T, Kane J, Wettstein PJ, Lanza RP, Studer L, Vrana KE, West MD. Parthenogenetic stem cells in nonhuman primates. Science 2002;295:819. [PubMed: 11823632]

Clarke DJ, Brundin P, Strecker RE, Nilsson OG, Bjorklund A, Lindvall O. Human fetal dopamine neurons grafted in a rat model of Parkinson's disease: ultrastructural evidence for synapse formation using tyrosine hydroxylase immunocytochemistry. Exp Brain Res 1988;73:115–126. [PubMed: 3145209]

Corbin JG, Rutlin M, Gaiano N, Fishell G. Combinatorial function of the homeodomain proteins Nkx2.1 and Gsh2 in ventral telencephalic patterning. Development 2003;130:4895–4906. [PubMed: 12930780]

Costantini LC, Snyder-Keller A. Co-transplantation of fetal lateral ganglionic eminence and ventral mesencephalon can augment function and development of intrastriatal transplants. Exp Neurol 1997;145:214–227. [PubMed: 9184123]

Dunnet S, Bjorklund A, Schmidt R, Stenevi U, Iverson S. Intracerebral grafting of neuronal cell suspensions. IV. Behavioral recovery in rats with unilateral 6-OHDA lesions in different brain sites. Acta Physiol Scand 1983;522:29–37.

Echevarria D, Vieira C, Gimeno L, Martinez S. Neuroepithelial secondary organizers and cell fate specification in the developing brain. Brain Res Brain Res Rev 2003;43:179–191. [PubMed: 14572913]

Emgard-Mattson M, Karlsson J, Nakao N, Brundin P. Addition of lateral ganglionic eminence to rat mesencephalic grafts affects fiber outgrowth but does not enhance function. Cell Transplant 1997;6:277–286. [PubMed: 9171160]

Foster GA, Schultzberg M, Hokfelt T, Goldstein M, Hemmings HC Jr, Ouimet CC, Walaas SI, Greengard P. Development of a dopamine-and cyclic adenosine 3′: 5′-monophosphate-regulated phosphoprotein (DARPP-32) in the prenatal rat central nervous system, and its relationship to the arrival of presumptive dopaminergic innervation. J Neurosci 1987;7:1994–2018. [PubMed: 2886563]

Fukuda H, Takahashi J, Watanabe K, Hayashi H, Morizane A, Koyanagi M, Sasai Y, Hashimoto N. Fluorescence-activated cell sorting-based purification of embryonic stem cell-derived neural precursors averts tumor formation after transplantation. Stem Cells 2006;24:763–771. [PubMed: 16223855]

Galpern WR, Burns LH, Deacon TW, Dinsmore J, Isacson O. Xenotransplantation of porcine fetal ventral mesencephalon in a rat model of Parkinson's disease: functional recovery and graft morphology. Exp Neurol 1996;140:1–13. [PubMed: 8682173]

Hemmendinger LM, Garber BB, Hoffmann PC, Heller A. Target neuron-specific process formation by embryonic mesencephalic dopamine neurons in vitro. Proc Natl Acad Sci USA 1981;78:1264–1268. [PubMed: 7015330]

Holm K, Isacson O. Factors intrinsic to the neuron can induce and maintain its ability to promote axonal outgrowth: a role for BCL2? Trends Neurosci 1999;22:269–273. [PubMed: 10354605]

Isacson O, Bjorklund LM, Schumacher JM. Toward full restoration of synaptic and terminal function of the dopaminergic system in Parkinson's disease by stem cells. Ann Neurol 2003;53(Suppl 3):S135–S146. [PubMed: 12666105]discussion S146–138

Isacson O, Deacon TW. Specific axon guidance factors persist in the adult brain as demonstrated by pig neuroblasts transplanted to the rat. Neuroscience 1996;75:827–837. [PubMed: 8951876]

Isacson O, Deacon TW, Pakzaban P, Galpern WR, Dinsmore J, Burns LH. Transplanted xenogeneic neural cells in neurodegenerative disease models exhibit remarkable axonal target specificity and distinct growth patterns of glial and axonal fibres. Nat Med 1995;1:1189–1194. [PubMed: 7584993]

Isacson, O.; Deacon, T.; Schumacher, J. Immunobiology and neuroscience of xenotransplantation in neurological disease. In: Tuszynski, M.; Kordower, J., editors. CNS Regeneration: Basic Science and Clinical Advances. Academic Press; San Diego: 1998. p. 365-387.

Johe KK, Hazel TG, Muller T, Dugich-Djordjevic MM, McKay RD, Vicario-Abejon C, Collazo D. Single factors direct the differentiation of stem cells from the fetal and adult central nervous system. Functions of basic fibroblast growth factor and neurotrophins in the differentiation of hippocampal neurons. Genes Dev 1996;10:3129–3140. [PubMed: 8985182]

Kim JH, Auerbach JM, Rodriguez-Gomez JA, Velasco I, Gavin D, Lumelsky N, Lee SH, Nguyen J, Sanchez-Pernaute R, Bankiewicz K, McKay R. Dopamine neurons derived from embryonic stem cells function in an animal model of Parkinson's disease. Nature 2002;418:50–56. [PubMed: 12077607]

Mandel RJ, Brundin P, Bjorklund A. The importance of graft placement and task complexity for transplant-induced recovery of simple and complex sensorimotor deficits in dopamine denervated rats. Eur J Neurosci 1990;2:888–894. [PubMed: 12106096]

Mendez I, Sanchez-Pernaute R, Cooper O, Vinuela A, Ferrari D, Bjorklund L, Dagher A, Isacson O. Cell type analysis of functional fetal dopamine cell suspension transplants in the striatum and substantia nigra of patients with Parkinson's disease. Brain 2005;128:1498–1510. [PubMed: 15872020]

Park CH, Minn YK, Lee JY, Choi DH, Chang MY, Shim JW, Ko JY, Koh HC, Kang MJ, Kang JS, Rhie DJ, Lee YS, Son H, Moon SY, Kim KS, Lee SH. In vitro and in vivo analyses of human embryonic stem cell-derived dopamine neurons. J Neurochem 2005;92:1265–1276. [PubMed: 15715675]

Paxinos, G.; Watson, C. The Rat Brain in Stereotaxic Coordinates. Academic Press; San Diego: 1986.

Perrier AL, Tabar V, Barberi T, Rubio ME, Bruses J, Topf N, Harrison NL, Studer L. Derivation of midbrain dopamine neurons from human embryonic stem cells. Proc Natl Acad Sci USA 2004;101:12543–12548. [PubMed: 15310843]

di Porzio U, Daguet J, Glowinski J, Prochiantz A. Effect of striatal cells on in vitro maturation of mesencephalic dopaminergic neurons grown in serum-free conditions. Nature 1980;288:370–373. [PubMed: 7432535]

Prochiantz A, Daguet MC, Herbet A, Glowinski J. Specific stimulation of in vitro maturation of mesencephalic dopaminergic neurones by striatal membranes. Nature 1981;293:570–572. [PubMed: 7290189]

Prochiantz A, DiPorzio U, Kato A, Berger B, Glowinski J. In vitro maturation of mesencephalic dopaminergic neurons from mouse embryos is enhanced in presence of their striatal target cells. Proc Natl Acad Sci USA 1979;76:5387–5391. [PubMed: 291955]

Reubinoff BE, Itsykson P, Turetsky T, Pera MF, Reinhartz E, Itzik A, Ben-Hur T. Neural progenitors from human embryonic stem cells. Nat Biotechnol 2001;19:1134–1140. [PubMed: 11731782]

Sanchez-Pernaute R, Studer L, Ferrari D, Perrier A, Lee H, Vinuela A, Isacson O. Long-term survival of dopamine neurons derived from parthenogenetic primate embryonic stem cells (cyno-1) after transplantation. Stem Cells 2005;23:914–922. [PubMed: 15941857]

Schultzberg M, Dunnett S, Bjorklund A, Stenevi U, Hokfelt T, Dockray G, Goldstein M. Dopamine and cholecystokinin immunoreactive neurons in mesencephalic grafts reinnervating the neostriatum: evidence for selective growth regulation. Neuroscience 1984;12:17–32. [PubMed: 6146944]

Schulz TC, Noggle SA, Palmarini GM, Weiler DA, Lyons IG, Pensa KA, Meedeniya AC, Davidson BP, Lambert NA, Condie BG. Differentiation of human embryonic stem cells to dopaminergic neurons in serum-free suspension culture. Stem Cells 2004;22:1218–1238. [PubMed: 15579641]

Simon HH, Bhatt L, Gherbassi D, Sgado P, Alberi L. Midbrain dopaminergic neurons: determination of their developmental fate by transcription factors. Ann NY Acad Sci 2003;991:36–47. [PubMed: 12846972]

Sortwell CE, Collier TJ, Sladek JR Jr. Co-grafted embryonic striatum increases the survival of grafted embryonic dopamine neurons. J Comp Neurol 1998;399:530–540. [PubMed: 9741481]

Stromberg I, Bjorklund L, Forander P. The age of striatum determines the pattern and extent of dopaminergic innervation: a nigrostriatal double graft study. Cell Transplant 1997;6:287–296. [PubMed: 9171161]

Takagi Y, Takahashi J, Saiki H, Morizane A, Hayashi T, Kishi Y, Fukuda H, Okamoto Y, Koyanagi M, Ideguchi M, Hayashi H, Imazato T, Kawasaki H, Suemori H, Omachi S, Iida H, Itoh N, Nakatsuji N, Sasai Y, Hashimoto N. Dopaminergic neurons generated from monkey embryonic stem cells function in a Parkinson primate model. J Clin Invest 2005;115:102–109. [PubMed: 15630449]

Tao W, Lai E. Telencephalon-restricted expression of BF-1, a new member of the HNF-3/fork head gene family, in the developing rat brain. Neuron 1992;8:957–966. [PubMed: 1350202]

Tessier-Lavigne M, Goodman CS. The molecular biology of axon guidance. Science 1996;274:1123–1133. [PubMed: 8895455]

Thompson L, Barraud P, Andersson E, Kirik D, Bjorklund A. Identification of dopaminergic neurons of nigral and ventral tegmental area subtypes in grafts of fetal ventral mesencephalon based on cell morphology, protein expression, and efferent projections. J Neurosci 2005;25:6467–6477. [PubMed: 16000637]

Vrana KE, Hipp JD, Goss AM, McCool BA, Riddle DR, Walker SJ, Wettstein PJ, Studer LP, Tabar V, Cunniff K, Chapman K, Vilner L, West MD, Grant KA, Cibelli JB. Nonhuman primate parthenogenetic stem cells. Proc Natl Acad Sci USA 2003;100(Suppl 1):11911–11916. [PubMed: 14504386]

Wang HF, Liu FC. Developmental restriction of the LIM homeodomain transcription factor Islet-1 expression to cholinergic neurons in the rat striatum. Neuroscience 2001;103:999–1016. [PubMed: 11301207]

Yan Y, Yang D, Zarnowska ED, Du Z, Werbel B, Valliere C, Pearce RA, Thomson JA, Zhang SC. Directed differentiation of dopaminergic neuronal subtypes from human embryonic stem cells. Stem Cells 2005;23:781–790. [PubMed: 15917474]

Ye W, Shimamura K, Rubenstein JL, Hynes MA, Rosenthal A. FGF and Shh signals control dopaminergic and serotonergic cell fate in the anterior neural plate. Cell 1998;93:755–766. [PubMed: 9630220]

Yurek DM, Collier TJ, Sladek JR Jr. Embryonic mesencephalic and striatal co-grafts: development of grafted dopamine neurons and functional recovery. Exp Neurol 1990;109:191–199. [PubMed: 2379555]

Yurek DM, Fletcher-Turner A. Comparison of embryonic stem cell-derived dopamine neuron grafts and fetal ventral mesencephalic tissue grafts: morphology and function. Cell Transplant 2004;13:295–306. [PubMed: 15191167]

Abbreviations

6-OHDA
6-hydroxydopamine

AA
ascorbic acid

AADC
aromatic amino acid decarboxylase

BDNF
brain-derived neurotrophic factor

Bf-1
brain factor 1

DA
dopamine

DARP
DA and cAMP-regulated phosphoprotein

DAT
dopamine transporter

ES
embryonic stem

FGF
fibroblast growth factor

Girk
G-coupled inward rectifier K^+ channel

HNA
human nuclear antigen

LGE
lateral ganglionic eminence

NCAM
neural cell adhesion molecule

NeuN
neuronal nuclei

NF70
: neurofilament 70

PBS
: phosphate-buffered saline

SHH
: sonic hedgehog

TH
: tyrosine hydroxylase

VM
: ventral midbrain

VMAT
: vesicular monoamine transporter

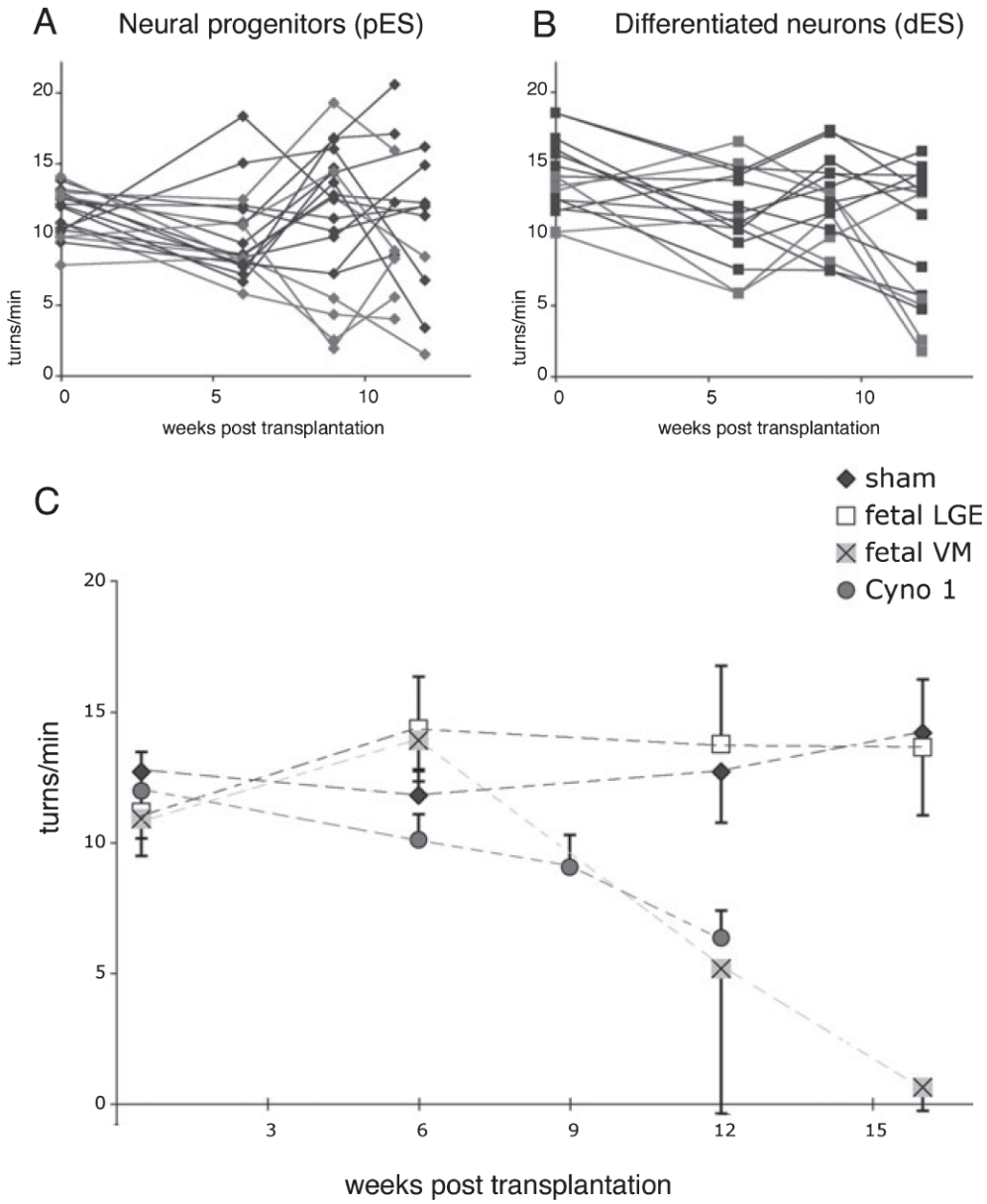

Fig. 1.

Amphetamine-induced rotation was evaluated before and (A) at 6, 9 and 11 weeks post-transplantation in animals grafted with Cyno-1 primate ES progenitors (pES, *in vitro* day 28) and (B) at 6, 9 and 12 weeks in animals grafted with Cyno-1 primate ES differentiated neurons (dES, *in vitro* day 42). The rotation scores of the animals with surviving grafts containing ≥ 200 TH + neurons are highlighted in red in (A) (pES, $n = 6$, 417 ± 79) and (B) (dES, $n = 7$, 425 ± 103), and shown averaged together in (C) with control transplantation groups: fetal primate midbrain [Fetal VM (ventral midbrain), blue, $n = 3$, 744 ± 456], served as positive control, fetal primate striatum [Fetal LGE (lateral ganglionic eminence), gray, $n = 4$] and animals with no grafts (sham, black, $n = 3$), which served as negative controls. Evaluation of D-amphetamine response showed a progressive reduction of motor asymmetry (ipsilateral turns/min) in animals receiving both pES and dES cells that had ≥ 200 TH + neurons at 12 weeks

compared with control animals (LGE and sham). Using regression analysis we found that the improvement was correlated with the number of TH + neurons ($r = 0.5$, $P < 0.05$). The primate fetal midbrain controls also improved as expected after a 16-week period.

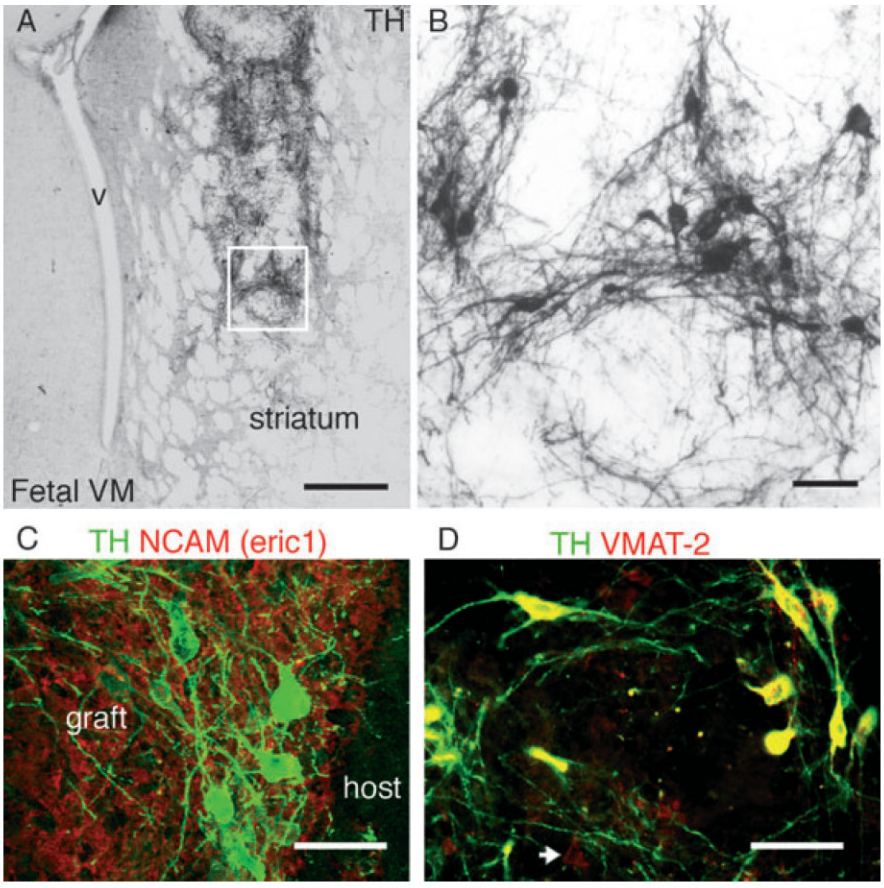

Fig. 2.

(A and B) Tyrosine hydroxylase (TH) immunoreactivity in a representative graft from primate fetal ventral midbrain at 16 weeks post-transplantation into the striatum of a hemi-parkinsonian 6-OHDA-lesioned rat. The boxed area is magnified in (B). (C) Primate cells in the graft were identified by the primate specific marker neural cell adhesion molecule (NCAM; eric 1, red), TH + (green) neurons within the graft were located in clusters, close to the host–graft interface, and (D) co-expressed the vesicular monoamine transporter (VMAT-2, red). VMAT-2 +/TH – neurons were also present in these grafts (arrow). V, ventricle; Scale bar: 500 μm (A); 50 μm (B–D).

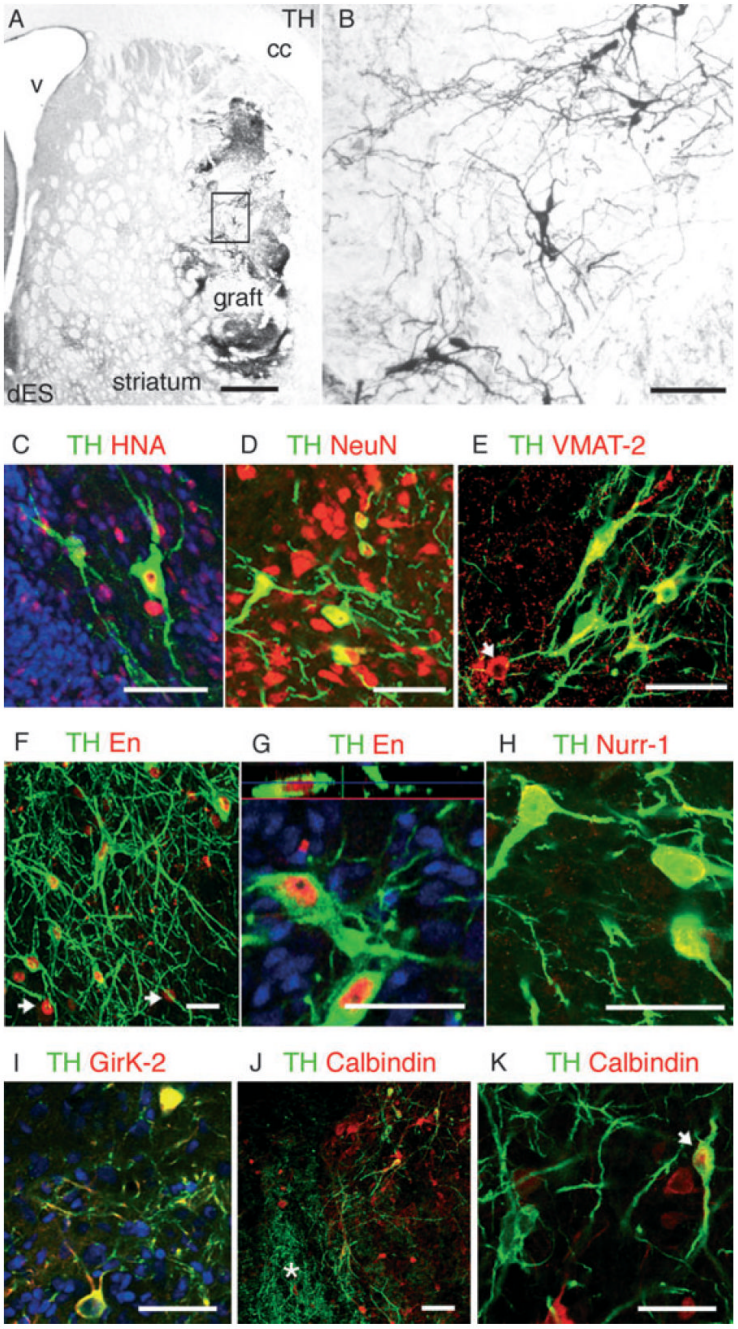

Fig. 3.

(A and B) Tyrosine hydroxylase (TH) immunoreactivity in a representative graft derived from differentiated primate ES cells (dES) showing TH + neurons within the graft (boxed area is magnified in B) and areas of dense TH neuritic arborization. (C) ES-derived TH + (green in C–K) neurons in the grafts expressed the primate-and human-specific nuclear antigen (HNA, red), (D) neuronal nuclear antigen (NeuN, red) and (E) vesicular monoamine transporter (VMAT-2, red). Like in the fetal grafts (Fig. 2D), VMAT-2 +/TH – cells were also found (arrow). (F) TH + neurons in dES grafts expressed the homeobox transcription factor Engrailed (En, red, 93 ± 3%) and ~45% of En + cells expressed TH (arrows in F point to En +/TH – cells) (G) Nuclear localization of En (red) in a TH + neuron is shown in an orthogonal reconstruction

of serial confocal optical sections. (H) Nurr1 (red) was also expressed by TH + neurons. (I) Some TH + neurons in the grafts co-expressed the G-coupled inward rectifier K^+ channel 2 (Girk-2, red), which is preferentially expressed by midbrain dopamine neurons in the substantia pars compacta. (J and K) Some TH + neurons co-expressed calbindin (red) (J, arrow in K), which is highly expressed in the A10 dopamine subpopulations. Calbindin +/TH – neurons were also found in the grafts, but not in the areas of dense TH innervation (asterisk in J, see Fig. 4). cc, corpus callosum; V, ventricle. Scale bars: 500 μm (A); 50 μm (B–K).

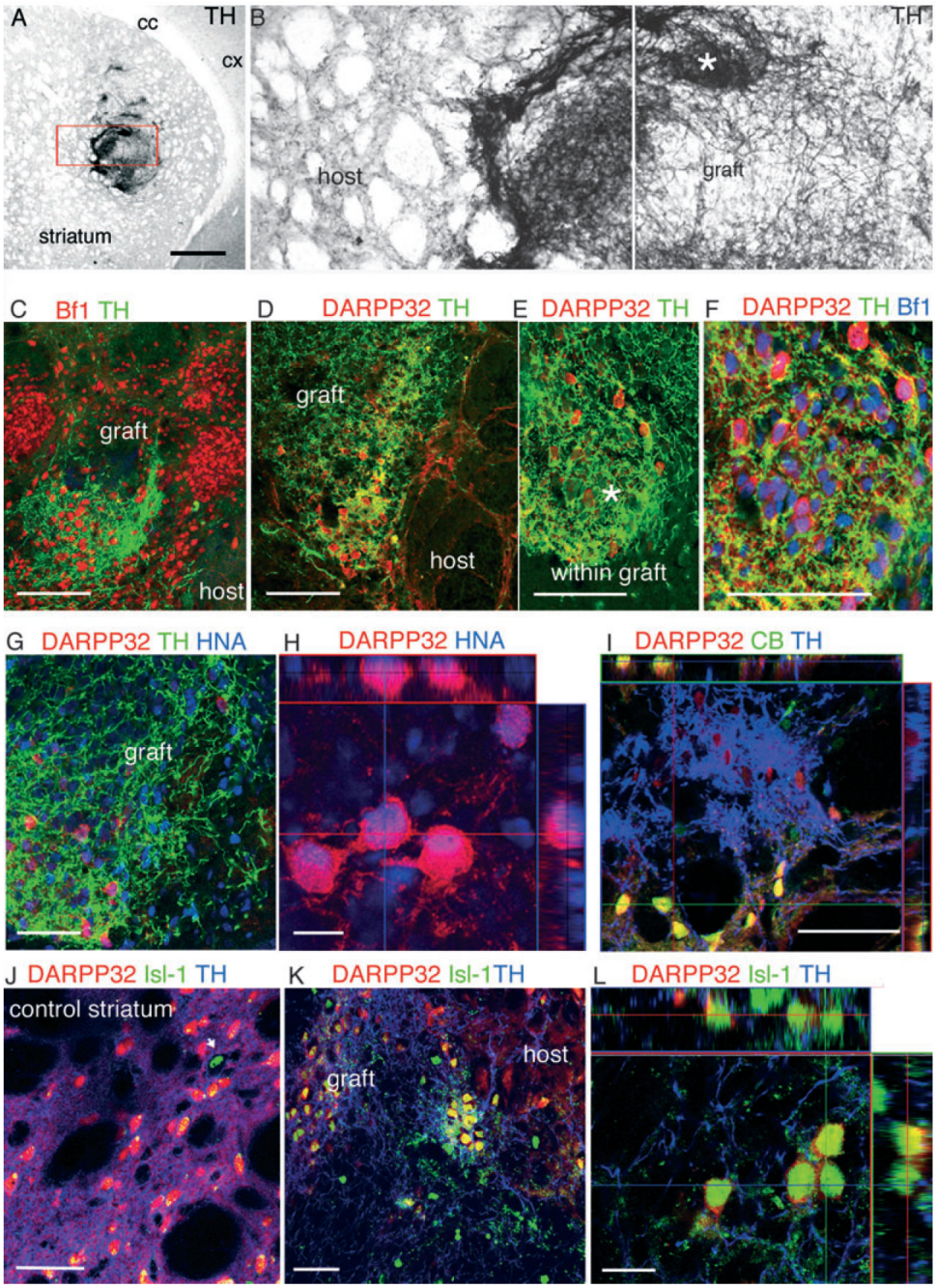

Fig. 4.

(A) Tyrosine hydroxylase (TH) immunoreactivity in the denervated striatum demonstrating patches of dense TH arborization within the graft. (B) Higher magnification of the boxed area in (A) shows the presence of some TH + fibers in the host, close to the graft border, and much denser areas (asterisk) within the graft. (C) Brain factor (Bf)-1 (red)-positive nuclei were found in both innervated and also in non-innervated areas within the graft. (D and E) Clusters of dopamine and cAMP-regulated phosphoprotein (DARPP)-32 + neurons (red in D–L) were found in densely innervated areas in all the grafts. (F) DARPP-32 + neurons co-expressed the forebrain transcription factor Bf-1 (blue). (G) These DARPP-32 + neurons were derived from the primate ES cells as shown by HNA (blue) nuclear expression. (H) Orthogonal

reconstruction of serial optical sections showing nuclear localization of HNA (blue) in a cluster of DARPP-32 + neurons. (I) These DARPP-32 + neurons were immature, as demonstrated by the absence of calbindin (green) co-expression, which is co-expressed by the mature DARPP-32 + neurons in the host (co-localization appears yellow in host neurons in the orthogonal confocal reconstruction). Within the graft less than 10% of DARPP-32 + neurons co-expressed calbindin. (J–L) A similar pattern was observed for co-expression of DARPP-32 and Islet (Isl-1, blue). In the adult host striatum Isl-1 is expressed by large cholinergic interneurons (arrow) but not by medium-size spiny neurons (DARPP-32 +). However, within the graft (K and L) DARPP-32 + neurons often co-expressed Isl-1 (blue). Scale bars: 500 μm (A); 10 μm (H and L); 50 μm (C–G, I–K).

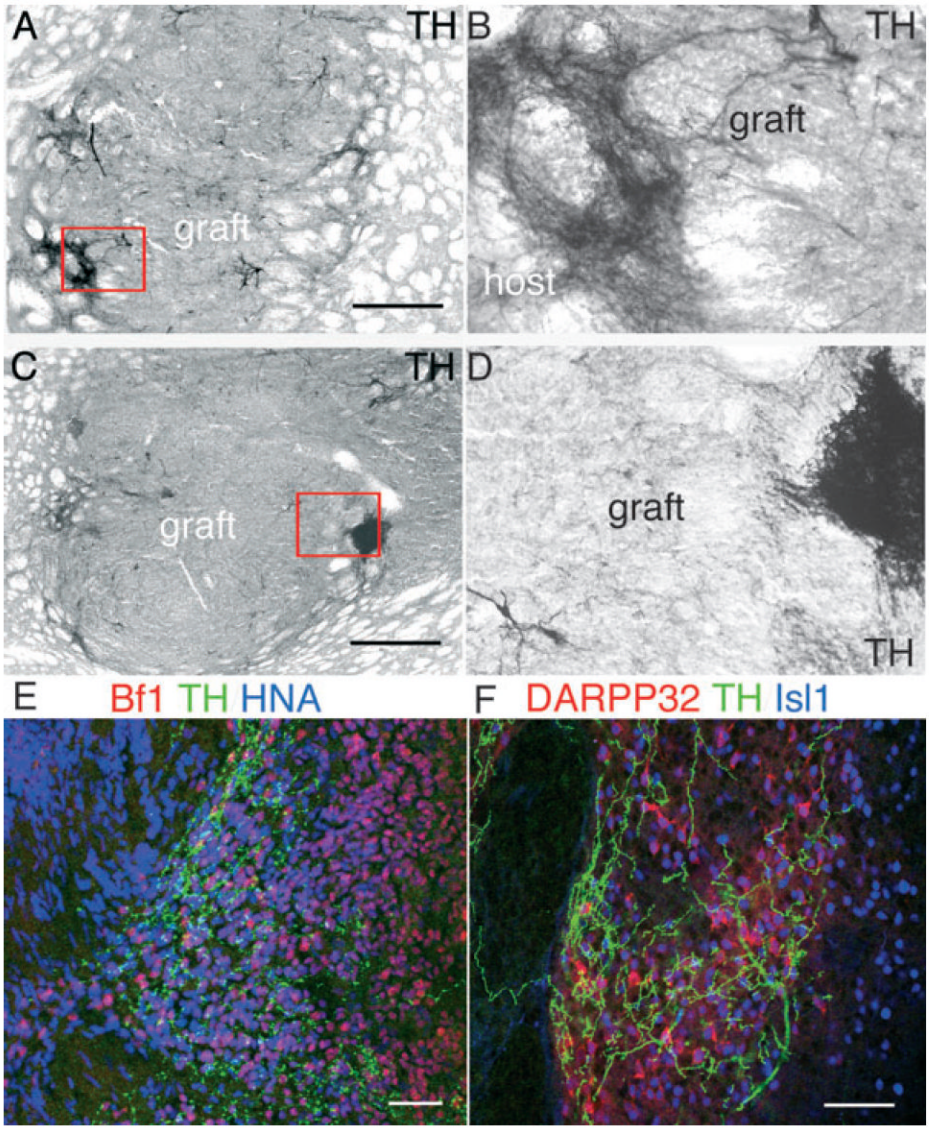

Fig. 5.

(A–D) Grafts derived from progenitors (pES, 28 days *in vitro*) showed a similar pattern of dense tyrosine hydroxylase (TH) innervation within defined areas of the graft. TH immunostaining revealed some limited outgrowth into the host (A, boxed area is magnified in B) and dense patches within the graft (C, boxed area magnified in D). (E) As in dES-derived grafts (Fig. 4), within the graft [human nuclear antigen (HNA) +, blue] TH fibers innervated brain factor (Bf)-1 + (red) neurons, and (F) coincided with clusters of dopamine and cAMP-regulated phosphoprotein (DARPP)-32 + (red)/Isl-1 + (blue) neurons. Scale bars: 500 μm (A and C); 50 μm (E and F).

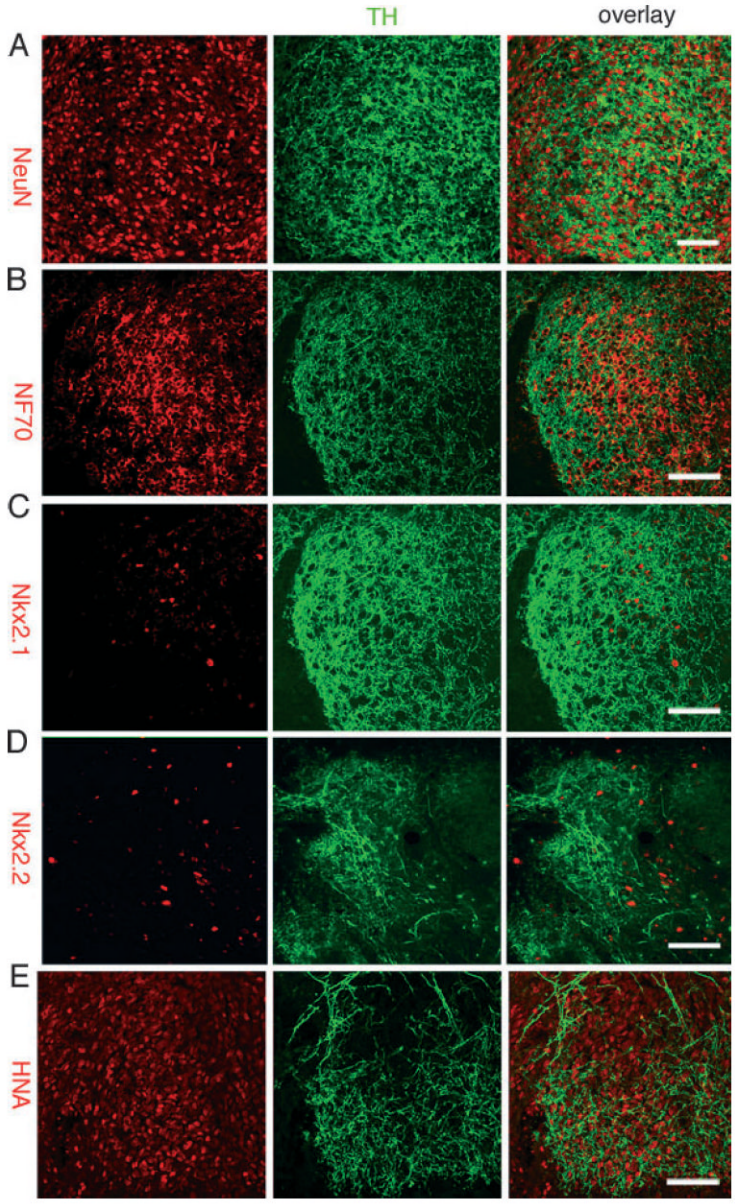

Fig. 6.

Most cells in the areas of the grafts with dense tyrosine hydroxylase (TH) innervation were neurons and expressed (A) neuronal nuclei (NeuN, red) and (B) neurofilament (NF70, red). (C and D) Because Bf-1 was highly expressed in such areas (Figs 4C and 5E), we examined the expression of other regional forebrain transcription factors including (C) Nkx2.1 (red), (D) Nkx.2.2 (red) and Pax6 (not shown), which failed to co-localize to TH + areas. (E) These areas were located within the graft and most cells expressed the primate-specific human nuclear antigen (HNA, red). Scale bars: 50 μm.

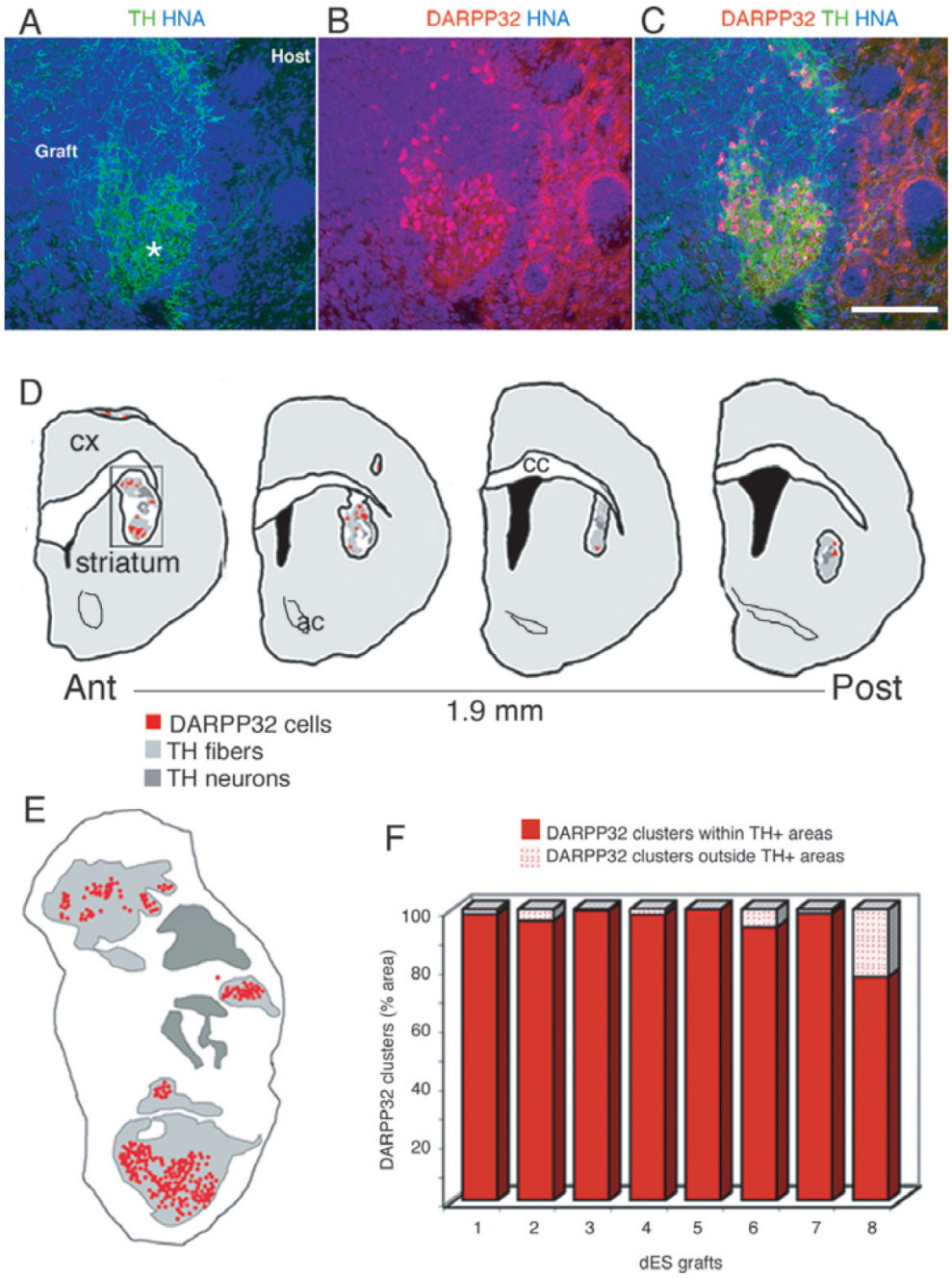

Fig. 7.

(A) Patches of dense tyrosine hydroxylase (TH) + (green) fibers within the graft [human nuclear antigen (HNA) +, blue] in a representative animal transplanted with dES. (B) Primate dopamine and cAMP-regulated phosphoprotein (DARPP)-32 + neurons (red, overlap with HNA appears purple) were found in clusters that (C) coincided with the areas of TH + innervation. (D and E) In order to quantify this distribution, DARPP-32 + neurons and TH + areas were mapped on serial sections (480 μm apart) spanning the whole graft in animals grafted with dES (*n* = 8): maps of a representative graft showing the distribution of DARPP-32 + neuronal clusters with respect to TH innervation. (E) Detail of the map boxed in (D): each red dot represents one primate DARPP-32 + neuron; the regions densely innervated by TH + fibers are outlined in

light gray (see A and Fig. 3B, asterisks), and the regions in dark gray delineate the areas where the TH + cell bodies are (for morphological delineation of these areas, see Fig. 3A and B). (F) Quantification of DARPP-32 + neurons distribution was done on each map, and the percentage of DARPP-32 + neurons present inside and outside TH-innervated areas is shown for each animal. Almost all (95 ± 2.7%) DARPP-32 + neurons were located within TH-innervated areas, supporting a strong attractive effect of DARPP-32 + neurons and TH + fibers. Scale bar: 150 μm.